Applied Clay Science 115 (2015) 67–75

Contents lists available at ScienceDirect

Applied Clay Science

journal homepage: www.elsevier.com/locate/clay

Fe_2O_3–palygorskite nanoparticles, efficient adsorbates for pesticide removal

Affaf Ouali [a], Lala Setti Belaroui [a,b,*], Abdelkader Bengueddach [a], Alberto Lopez Galindo [c], Aránzazu Peña [c]

[a] Laboratory of Chemistry of Materials (LCM), Faculty of Applied and Exact Sciences, University of Oran 1, BP 1524 Oran El M'Naouer, Oran, Algeria
[b] Department of Pharmacy, Faculty of Medicine, University of Oran 1, BP 1510 Oran El M'Naouer, Oran, Algeria
[c] Instituto Andaluz de Ciencias de la Tierra (CSIC—University of Granada), Avda. de las Palmeras, 4, 18100 Armilla, Granada, Spain

ARTICLE INFO

Article history:
Received 27 April 2015
Received in revised form 22 June 2015
Accepted 16 July 2015
Available online xxxx

Keywords:
Palygorskite
Iron oxide
Adsorption
Fenarimol

ABSTRACT

Recently, magnetic adsorbents have aroused a significant attention because of their excellent adsorption capacity. An Algerian palygorskite/magnetic iron oxide was prepared by chemical co-precipitation and characterized using infrared spectroscopy, X-ray diffraction and X-ray fluorescence. The results prove the formation of a red brick powder, with magnetic character, showing a high percentage of iron oxide on palygorskite. To verify the ability of the magnetic palygorskite for retaining organic pollutants, three different samples were evaluated for the adsorption of the fungicide fenarimol from aqueous samples: sifted palygorskite, purified palygorskite and Fe_2O_3/palygorskite. The effects of different variables were assessed: adsorbent mass, reaction time, initial pesticide concentration and desorption stability. Fenarimol adsorption kinetics followed a pseudo-second order model. The adsorption rates were 11%, 50% and 70%, for sifted, purified and Fe_2O_3/palygorskite, respectively. Both Langmuir and Freundlich models could be used to describe fenarimol adsorption on sifted and purified palygorskites. However only the Freundlich model could fit the adsorption data on Fe_2O_3/palygorskite, probably due to the adsorbent heterogeneity. Stability of fenarimol desorption from the three samples, where the fungicide had been previously preadsorbed, showed that the extent of desorbed fenarimol from Fe_2O_3/palygorskite remained constant along the studied period (15 days).

1. Introduction

Pesticides are organic substances intended to protect crops. For more than half a century these compounds have been considerably used by intensive agriculture leading to an important environmental pollution (water, air, soil and food) that can negatively affect public human health.

Fenarimol is a systemic fungicide with protectant, curative and eradicating properties belonging to the substituted pyrimidines. It is applied against powdery mildew and black spot in fields and greenhouses of ornamental plants and horticultural crops such as strawberries, vineyards, tomatoes, peppers and eggplants (Tomlin, 2003; Cabizza et al., 2012). Its use in horticultural production poses an environmental risk because residues of this pesticide can be found in plants (Peña et al., 2014), in soil or move from the soil by leaching or runoff to surface or groundwater (Wightwick et al., 2012; Rodríguez-Liébana et al., 2014a,b). The presence of pesticides in water bodies requires therefore specific actions for their removal, implying a major environmental concern.

The removal of pesticides from water has been approached by adsorption on different substrates. Fenarimol, together with imazaquin and oxadiazon, was retained on inorganic materials derived from zeolites, diatomaceous earths and fired clays (Wehtje et al., 2000) and different pesticides or pharmaceuticals on activated carbon (Hameed et al., 2009; Shaarani and Hameed, 2010), on various natural clay minerals (Fernandes de Oliveira et al., 2005; Li et al., 2006; Azejjel et al., 2009; Peng et al., 2009; Rivagli et al., 2014) and organoclays (Azejjel et al., 2009; Saha et al., 2013). Fenarimol is known to have androgenic effects on some vertebrates and mollusks (Watermann et al., 2013) and may possibly alter normal reproductive function of offspring's in humans and wildlife (Park et al., 2011). However, it has been classified as slightly hazardous (Class III) according to the WHO pesticide classification (World Health Organization, 2009) based on acute oral LD_{50} values, set for this fungicide as 2500 mg kg^{-1}.

An innovative system to retain pesticides present in water can be the use of Algerian palygorskite (Pal) before and after modification with magnetic iron oxides. These nanoparticles have been developed by co-precipitation, the most common and productive method in terms of powder quantity. The protocol of this method has been done by

* Corresponding author at: Laboratory of Chemistry of Materials (LCM), Faculty of Applied and Exact Sciences, University of Oran 1, BP 1524 Oran El M'Naouer, Oran, Algeria.
E-mail addresses: lalasettibelaroui@yahoo.fr, belaroui.lalasetti@univ-oran.dz (L.S. Belaroui).

http://dx.doi.org/10.1016/j.clay.2015.07.026
0169-1317/

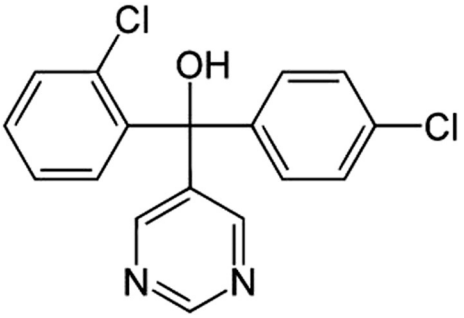

Fig. 1. Chemical structure of the fungicide fenarimol.

Massart (1982) and adapted by Mornet et al. (2000) and a few others (Grasset et al., 2001, 2002; Daou et al., 2006; Fu et al., 2011). This protocol allows obtaining the nanoparticles in great quantity with a good reproduction of size and structure (Fauconnier, 1996; Lefebvre, 1996).

Palygorskite, called attapulgite in trade circles, has an ideal formula of $(Mg,Al)_5Si_8O_{20}(OH)_2(H_2O)_4 \cdot 4H_2O$. It is a magnesium aluminum non-planar hydrous 2:1 phyllosilicate with modulated structure, showing a fibrous morphology resulting from the 180° inversion occurring every four silicon tetrahedra, which produces a structure of chains aligned parallel to the "a" axis, each of which has a 2:1 type structure, with exchangeable cations and reactive Si–OH groups on its surface (Bradley, 1940; Serratosa, 1978; Suarez Barrios et al., 1995) that may be involved in interactions with many different compounds. The alternation of these building blocks creates structural cavities (zeolitic channels) that lead palygorskite to have great internal surface (Casal et al., 2001). The width of the block structure is 0.64 to 0.37 nm (Fernández-Saavedra et al., 2004).

The objective of the present study was a) to characterize raw and modified Pal, b) to assess the ability of raw and modified Pal for removing fenarimol from aqueous solutions and c) to optimize the conditions for its adsorption. The equilibrium and kinetics of adsorption, the thermodynamic parameters and the stability of desorption were also investigated. Various mathematical models were used to fit the experimental data.

2. Materials and methods

2.1. Chemicals and reagents

In East Algeria, near the city of El Ghoufi, some Tertiary sediments include palygorskite. Two samples were used: the first one (Sif Pal), rich in dolomite (Belaroui et al., 2014), was ground and sieved to 90 μm mesh size, and the second one (Pur Pal) was chemically treated according to the protocol of Dali Youcef (2012) with HCl 4 N at room temperature.

A standard of the fungicide fenarimol [(±)-2,4′-dichloro-α(pyrimidin-5-yl)benzhydryl alcohol] (Dr. Ehrenstorfer, Germany, purity ≥98%) was used without further purification (Fig. 1). Its octanol/water partition coefficient (log K_{ow}) is 3.69, and its solubility in water is 13.7 mg L^{-1} (Tomlin, 2003). Stock standard solutions of fenarimol were prepared at 1 g L^{-1} in acetonitrile and diluted with high purity MilliQ water (Millipore, Bedford, MA).

Hexahydrate ferrite chloride ($FeCl_3 \cdot 6H_2O$), ferrous chloride tetrahydrate ($FeCl_2 \cdot 4H_2O$), ammonium hydroxide (NH_4OH, 34% of ammonia), hydrochloric acid (HCl, 37%), nitric acid (HNO_3, 66%) and acetone are reagents of analytic quality received from Prolabo® (France) and used without any further purification. HPLC grade acetonitrile (Prolabo) was also used.

2.2. Synthesis of Fe_2O_3-Pal nanoparticles

The nanoparticles were prepared by dissolving iron (II) and iron (III) chlorides in hydrochloric acid (1 N) at a 3/10 ratio, then mixing for a few minutes. The mixture was co-precipitated by the addition, under vigorous shaking, of 10 mL of ammonia at room temperature; afterwards 18.3 mL of nitric acid was added. Distilled water was then added to remove the acids and bases in excess. The red magnetic iron oxide was added to 1% mass dispersion of Pur Pal, maintaining the mixture under vigorous shaking for a few hours. The nanoparticles, dried up at 80 °C, are called Fe_2O_3-Pal.

2.3. Characterization of the nanoparticles

Infrared spectroscopic measurements were done on an Alpha-Bruker spectrophotometer using the KBr pellet method (1 mg per 150 mg sample), with a scan interval from 4000 to 400 cm^{-1}.

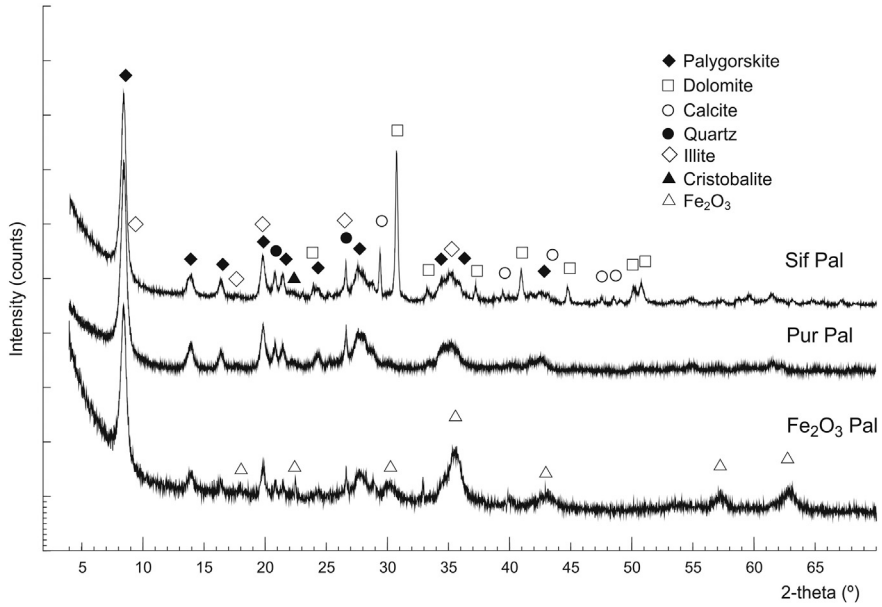

Fig. 2. X-ray diffraction patterns of Sif Pal, Pur Pal and Fe_2O_3 Pal samples.

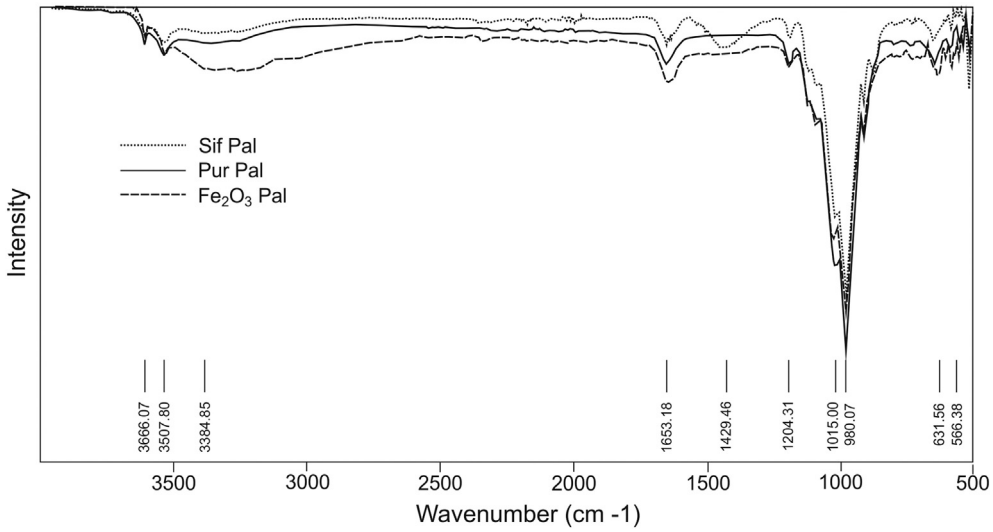

Fig. 3. IR spectra of Sif Pal, Pur Pal and Fe_2O_3 Pal samples.

The X-ray Powder Diffraction (XRPD) pattern of the sample was obtained by using a PANalytical X-Pert Pro diffractometer with Cu Kα radiation (45 kV, 40 mA), Ni filter, RTMS X'Celerator detector, 4°–70° scan range, 0.0084° step size, 10.150 s counting time, for a total of 7898 points and 11 min/sample.

Chemical sample analysis was performed with dispersive X-ray fluorescence (SpectraPLUS, S4 Pioneer, BRUKER) equipped with an Rh anode X-ray tube (60 kV, 150 mA).

pH (Eutech Instruments Cyberscan pH 2100, Singapore) and electrical conductivity (EC) (XS Instruments COND 510, Italy) were measured in sample/deionized water dispersion 1/2.5 (w/v).

To determine cation exchange capacity (CEC) clay powders (1 g) were dispersed in 25 mL tetramethylammonium bromide (1 M) aqueous solution, in order to displace their constituent cations. Dispersions were shaken overnight at 50 rpm in water bath at 25 ± 1 °C and then filtered. Cations in solution were individually assayed by atomic absorption (Na^+, Ca^{2+}, Mg^{2+}) or atomic emission (K^+) spectroscopy (PerkinElmer spectrophotometer 5100) and CEC was calculated as the sum of exchangeable cations, expressed in $meq_+/100$ g dry clay. Total C and S were analyzed by a carbon/sulfur analyzer (EMIA 920 V2, Horiba). Organic C (OC) was determined by a modified Walkley and Black method (Mingorance et al., 2007).

2.4. Adsorption kinetics

Pesticide adsorption kinetics was carried out using the batch equilibration system by mixing, in an end-over-end shaker (20 °C and natural clay pH), 20 mL of an aqueous solution of fenarimol at a constant concentration (5 mg L^{-1}) with 0.2 g adsorbent from 5 to 1320 min. Samples were centrifuged at 2800 rpm for 2 min and an aliquot of the corresponding supernatants was analyzed for pesticide concentration.

Pseudo-first, pseudo-second order and intraparticle diffusion kinetic equations were employed for the fitting of the experimental data. The pseudo-first-order model (Lagergren, 1898) was established for the liquid phase adsorption and is applicable only during the first minutes of the adsorption phenomenon. In this model the adsorption rate at time t is proportional to the difference between the adsorbed amount at equilibrium (X_e) and at time t (X_t), and can be expressed as:

$$\frac{\partial X_t}{\partial t} = k_1 (X_e - X_t) \quad (1)$$

where X_t and X_e are the adsorbed amounts (μg g^{-1}) at time t (min) and at equilibrium, respectively and k_1 is the rate constant of the pseudo-first-order process (min^{-1}).

The pseudo-second order model is generally used to describe adsorption phenomena such as chemisorption (Ho et al., 1996; Ho and McKay, 2000). It allows characterizing the adsorption kinetics taking into account both the case of rapid attachment of solutes on the most reactive sites and slow binding to the low energy sites (Travis and Entier, 1981). It is represented by the following equation:

$$\frac{\partial X_t}{\partial t} = k_2 (X_e - X_t)^2 \rightarrow \frac{\partial X_t}{(X_e - X_t)^2} = k_2 \partial t \quad (2)$$

where k_2 is the kinetic rate constant of the pseudo-second-order model (g μg^{-1} min^{-1}).

The intraparticle diffusion model (Weber and Morris, 1963) was also tested according to the following equation to evaluate the contribution of intra-particle diffusion mechanism:

$$X_t = C_I + k_p \times t^{1/2} \quad (3)$$

where C_I (μg g^{-1}) is a constant proportional to the boundary layer thickness and k_p is the intraparticle rate constant (μg g^{-1} $min^{1/2}$).

Table 1
Properties of raw and modified Algerian palygorskites.

	Sif Pal	Pur Pal	Fe_2O_3 Pal
pH	8.42	4.56	2.80
CEC ($meq_+/100$ g)	18.4	20.8	8.3
Total C (%)	3.4	0.2	1.2
Total S (%)	0.3	0.1	0.05
Organic C (%)	0.16	0.15	0.53
SiO_2 (g/100 g)	40.3	55.8	13.6
Al_2O_3 (g/100 g)	8.9	11.5	2.8
MgO (g/100 g)	8.9	8.0	1.8
Fe_2O_3 (g/100 g)	3.3	3.8	39.0
CaO (g/100 g)	9.7	0.11	0.25
MnO (g/100 g)	0.1	0.04	0.03
Na_2O (g/100 g)	0.2	0.03	0.1
K_2O (g/100 g)	0.9	1.1	0.4
TiO_2 (g/100 g)	0.4	0.6	0.2
P_2O_5 (g/100 g)	0.1	0.03	0.01
Cl (g/100 g)	<0.1	0.2	6.7
LOI	26.6	18.7	36.4

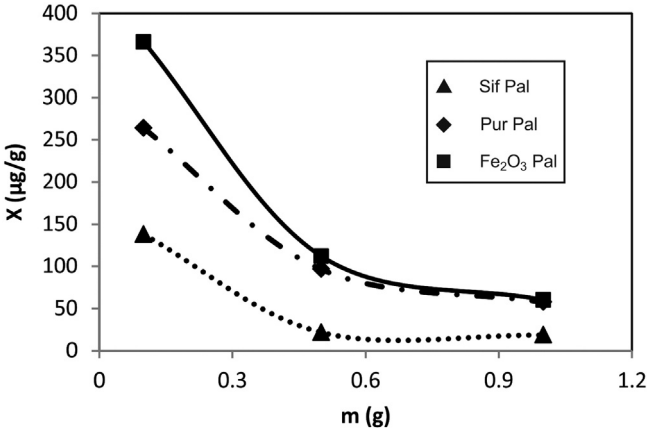

Fig. 4. Effect of adsorbent mass on fenarimol adsorption on Sif Pal, Pur Pal and Fe_2O_3 Pal.

2.5. Adsorption experiments

2.5.1. Effect of initial Pal mass

The batch equilibration method was also used for the isotherms. Samples (0.01–1.0 g) were weighed per duplicate into 30 mL Pyrex centrifuge tubes to which 20 mL of an aqueous pesticide solution at a concentration of 5 mg L^{-1} was added. After 24 h end-over-end shaking (20 ± 1 °C) the samples were treated as described for the kinetic studies.

2.5.2. Effect of initial pesticide concentration

Samples (0.2 g) were weighed per duplicate into 30 mL Pyrex centrifuge tubes to which 20 mL of an aqueous pesticide solution at concentrations ranging from 0.5 to 10 mg L^{-1} was added. After shaking in an end-over-end shaker (20 ± 1 °C) for 360 min (Sif Pal and Fe_2O_3 Pal) and for 960 min (Pur Pal), a sufficient time according to the preliminary kinetic studies, the samples were treated as described above. In all cases a blank without adsorbent was run to rule out possible pesticide losses due to degradation, volatilization or adsorption on tube walls. The 0.5% acetonitrile content should not have any effect on pesticide adsorption (Kibbey and Hayes, 1993).

2.5.3. Fitting to different mathematical models

To describe the adsorption equilibria, two commonly used mathematical expressions were applied to the experimental data, the Freundlich and Langmuir isotherm models. The Langmuir model (Langmuir, 1918) was originally developed to explain chemisorption on well-defined localized adsorption sites with identical adsorption energies. This model also assumes that adsorption is independent from the surface coverage and interaction between adsorbed molecules does not occur. Maximum adsorption is achieved when the surface of the adsorbent is covered with a monolayer of adsorbate. The Langmuir isotherm is expressed as follows:

$$X_e = \frac{X_{max} \times K_L \times C_e}{1 + K_L \times C_e} \quad (4)$$

where X_e represents the amount of fenarimol adsorbed per unit adsorbent (µg g^{-1}), X_{max} is the maximum adsorbed amount (µg g^{-1}), C_e is the equilibrium concentration of fenarimol in solution (mg L^{-1}) and K_L (L mg^{-1}) is the Langmuir constant which is related to equilibrium constant of adsorption. A dimensionless constant, the separation factor (R_L), calculated as

$$R_L = \frac{1}{1 + K_L \times C_0} \quad (5)$$

is used as an indication that adsorption is either unfavorable ($R_L > 1$), linear ($R_L = 1$), favorable ($0 < R_L < 1$) or irreversible ($R_L = 0$).

The Freundlich adsorption isotherm (Freundlich, 1906) gives an empirical expression encompassing an exponential distribution of active sites. The model considers either monolayer or multilayer adsorption, irrespective of the adsorbate concentration, and assumes that the adsorbent surface is energetically heterogeneous. The Freundlich isotherm is expressed as follows:

$$X = K_f \times C_e^{1/n} \quad (6)$$

where X and C_e are as indicated in the Langmuir isotherm, K_f is the Freundlich adsorption coefficient ($mg^{1-1/n}$ $mL^{1/n}$ kg^{-1}) and reflects the adsorption capacity, and 1/n is a dimensionless constant related to the energetic heterogeneity of adsorption sites.

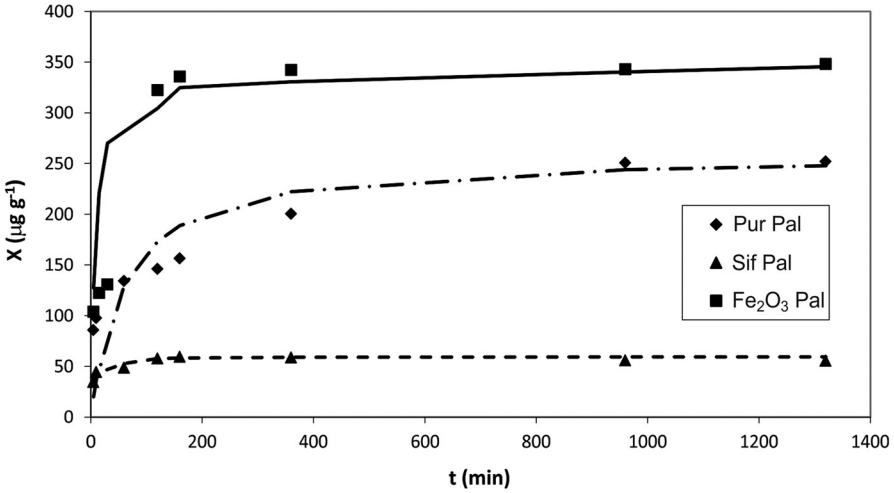

Fig. 5. Adsorption kinetics of fenarimol on Sif Pal, Pur Pal and Fe_2O_3 Pal.

Table 2
Parameters for the fitting to pseudo-first order, pseudo-second order and intraparticle diffusion kinetic models of fenarimol adsorption on raw and modified Algerian palygorskites.

	Clays		
	Sif Pal	Pur Pal	Fe_2O_3 Pal
$X_{max\ exp}$ (μg g^{-1})	55.7 ± 0.3	251 ± 1	344 ± 3
Pseudo-first order model:			
X_{max} (μg g^{-1})	14 ± 5	189 ± 11	95 ± 29
$k_1 \times 10^3$ (min^{-1})	9.5 ± 2.4	5.0 ± 0.3	3.9 ± 0.2
R^2	0.785	0.975	0.484
Pseudo-second order model:			
X_{max} (μg g^{-1})	59.6 ± 0.5	259 ± 14	348 ± 3
$k_2 \times 10^5$ (g μg^{-1} min^{-1})	435 ± 144	6.5 ± 2.3	33 ± 16
R^2	0.999	0.982	0.999
Intraparticle model:			
C_I (μg g^{-1})	28	76	22
k_{pI} (μg g^{-1} $min^{-1/2}$)	3.9	6.6	26.1
R^2	0.796	0.989	0.938
C_{II} (μg g^{-1})	60	243	332
k_{pII} (μg g^{-1} $min^{-1/2}$)	−0.13	0.24	0.43
R^2	0.769	1	0.834

2.6. Thermodynamic studies

The studies concerning the effect of temperature on the adsorption of fenarimol on the different samples are given by the Van't Hoff equation, where ΔH (kJ mol^{-1}), ΔS (kJ mol^{-1} K^{-1}) and ΔG (kJ mol^{-1}) are the enthalpy, entropy and the Gibbs free energy, respectively.

2.7. Adsorbent fortification and desorption stability

Adsorbent samples were fortified as in Rodríguez-Liébana et al. (2014b) by adding 0.5 mL of a fenarimol solution at 1 g L^{-1} in acetonitrile to 1.5 g of sample to give a nominal initial pesticide concentration of 0.33 mg g^{-1} (dry weight). Fortified samples were transferred to glass bottles and homogenized by shaking for one day at 20 °C in the darkness (Hernández-Soriano et al., 2012). Afterwards, samples were stored (4 °C) for subsequent analysis.

The stability of pesticide desorption was assessed during two weeks by batch double tests. An aliquot of 0.1 g of pesticide-fortified samples was placed in a 30 mL Pyrex centrifuge glass tube to which 10 mL MilliQ water was added. After 24 h shaking at 20 °C, the supernatants were centrifuged at 2500 rpm for 2 min and analyzed by HPLC.

2.8. Pesticide analysis

The concentration of fenarimol in the supernatants was determined by HPLC-DAD (LaChrom Ultra, Hitachi). A 20-μL sample, after filtration by PVDF filters (0.45 μm), was injected into a Zorbax Eclipse XDB-C18 column (Agilent, 2.1 × 150 mm, 5 μm ∅), protected by a precolumn (Vici, 0.115″ diam. × 0.028″, 0.5 μm ∅) at a flow rate 0.2 mL min^{-1}, the mobile phase consisting of a 50:50 (v:v) mixture of acetonitrile/MilliQ water and wavelength detection at 220 nm. Calibration was performed by triplicate injection of standard fenarimol solutions between 0.1 and 10 mg L^{-1} ($R^2 = 0.998$). Under these conditions the retention time of fenarimol was 6.8 min.

2.9. Statistical analysis

The equation that best fitted the experimental data was obtained by using non-linear regression with the Marquardt algorithm, which minimizes the sum of the squared differences between the observed and predicted values. The values of the determination coefficient (R^2) and of the standard error of the estimate were used to establish the goodness of fit. The relationship between variables was performed by correlation analysis. SPSS 17.0 software package was used.

3. Results and discussion

3.1. Characterization of the adsorbents

The XRD patterns of Sif Pal, Pur Pal and Fe_2O_3 Pal, and the main reflections of the different identified phases are shown in Fig. 2. Sample Sif Pal is mainly made up of palygorskite (69%) and dolomite (19%); lesser amounts of calcite (6%), quartz (3%), illite (3%) and traces of cristobalite have also been found. Sample Pur Pal is made up of palygorskite (91%), illite (5%), quartz (4%) and traces of critobalite. In sample Fe_2O_3 Pal, besides the cited minerals, magnetite and/or maghemite have also been identified (both minerals have similar diffraction patterns).

The IR spectrum of the Pur Pal showed the band at 3666 cm^{-1} corresponding to Mg–OH vibration and the band at 3507 cm^{-1} assigned to the vibrations of water coordinated to the Mg^{2+} ions located at the edges of the structural blocks (Fig. 3). As shown in Fig. 3, the bands at 3666 and 3501 cm^{-1} disappeared after the iron oxide coating process. They were replaced by a broad band at 3490 cm^{-1} which corresponds to the coordination of water. This result shows that Mg^{2+} cations were removed losing the water and hydroxyl group coordinated to them during the oxide coating process. This corresponds to the Mg^{2+} cations located at the edges of the octahedral layers. The increase in intensity of the hydroxyl vibration of the zeolitic water (1647 cm^{-1}) indicates that the iron oxide particles have not replaced the zeolitic water (Fig. 3). The bands at 1204 and 1015 cm^{-1} form as a result of the Si–O vibrations. Noticeable changes were also detected for bands in the region between 850 and 400 cm^{-1}, after the iron oxide coating process. These changes result in the conversion of several strips in one broadband.

The chemical composition of the samples is shown in Table 1. Sif Pal shows a strong magnesic–calcic character (8.9% of MgO and 9.7 of CaO) as a consequence of the presence of dolomite and calcite (Fig. 2). When these two minerals are eliminated in Pur Pal, SiO_2 and Al_2O_3 contents consequently increase. The treatment with the Fe^{2+} and Fe^{3+} nanoparticles resulted in an increase of Fe_2O_3 oxides in Fe_2O_3 Pal (Table 1), as expected.

The CEC ranged between approximately 8 meq_+ 100 g^{-1} for Fe_2O_3 Pal and 21 meq_+ 100 g^{-1} for Pur Pal. The CEC measured in pure Fe_2O_3 is 3.8 meq_+ 100 g^{-1}.

Table 3
Parameters of the fitting to Langmuir and Freundlich equations for the adsorption of fenarimol on raw and modified Algerian palygorskites.

Clays	Langmuir				Freundlich			
	K_L (L mg^{-1})	X_{max} (μg g^{-1})	R_L	R^2	K_f (μg^{1-n} mL^n g^{-1})	1/n	K_d (mL g^{-1})	R^2
Sif Pal	0.16 ± 0.06	70 ± 12	0.93	0.937	11 ± 2	0.62 ± 0.09	5.9	0.904
Pur Pal	0.59 ± 0.18	66 ± 6	0.77	0.887	30 ± 4	0.37 ± 0.08	10.8	0.772
Fe_2O_3 Pal	non				9 ± 1	1.69 ± 0.06	27.8	0.994

K_d is the distribution coefficient calculated for a C_e of 5 mg L^{-1}.
non: The data do not fit the corresponding mathematical model.

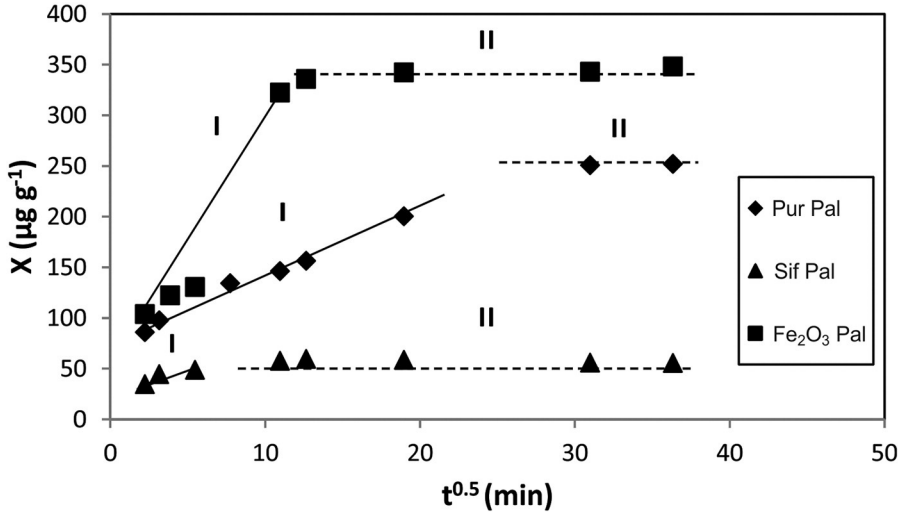

Fig. 6. Intraparticle diffusion plot for the adsorption of fenarimol on Sif Pal, Pur Pal and Fe_2O_3 Pal.

3.2. Adsorption kinetics and adsorption isotherms

3.2.1. Effect of adsorbent mass

Adsorbent dosage indicates the adsorption capacity of the different adsorbents for a given initial concentration and shaking time. The adsorption of fenarimol achieves a maximum with 500 mg of sample (Fig. 4), above which adsorption plateau is reached. However, due to the adsorbent availability and because the errors associated with weighing a sample mass ≤100 mg were too big, the adsorbent mass employed in the rest of experiments was 200 mg.

3.2.2. Adsorption kinetics

Adsorption kinetics for fenarimol in the three samples can be described by the same pattern (Fig. 5): an initially rapid process, reaching equilibrium in the first hours of contact, followed by a slower adsorption, which corresponds to less accessible sites (Table 2 and Fig. 5). The results from the kinetic study show that the maximum retained pesticide (X_{max}) corresponds to Fe_2O_3 Pal, then to Pur Pal, followed at a greater distance by Sif Pal.

The determination coefficients obtained from the fitting to a pseudo-first order kinetic model were not satisfactory (R^2 as low as 0.484) and the calculated X_{max} values differed greatly from the experimental values (Table 3). Experimental data were better fitted to a pseudo-second order kinetic equation ($R^2 \geq 0.982$, in all cases) and the difference between experimental and calculated X_{max} values ranged between 1.1 and 6.5%, reflecting a closer agreement, and in accordance with previous results concerning adsorption kinetics of pesticides or other organic compounds (Chen and Zhao, 2009; Saha et al., 2013). Furthermore an inverse relationship was found ($r = -0.930$) between adsorption kinetic rates and maximum pesticide adsorbed, in line with previous reported results (Fernández-Bayo et al., 2008; Villaverde et al., 2009).

In order to gain insight into the mechanisms controlling adsorption, the data from fenarimol kinetics were also fitted to the Weber's intraparticle diffusion (Weber and Morris, 1963). If the fitting to the Weber equation is linear and passes through the origin, the intraparticle diffusion is the sole rate-limiting step. However, very frequently, the plot of X versus $t^{1/2}$ is multi-linear, pointing to the existence of several steps in the adsorption process (El Bakouri et al., 2009). Two different stages were identified (Fig. 6): In the first one (I) the adsorbate molecules rapidly enter transporting pores (macropores and wider mesopores) and then penetrate more slowly in smaller pores (second stage, II).

In the first part of the plot the adsorption rates (kp_I) were ranged as Fe_2O_3 Pal ≫ Pur Pal ≥ Sif Pal (Table 3). The values of C_I indicate that the boundary layer diffusion effect is lower for Fe_2O_3 Pal and Sif Pal than for Pur Pal (Table 2). Adsorption rates in the second stage (kp_{II}) were much lower in all cases showing that diffusion into micropores is the rate-limiting process. Fig. 6 indicates that for Sif Pal and Fe_2O_3 Pal a rapid diffusion occurs, followed by a slowdown in the adsorption process corresponding to the diminution of pesticide concentration in the solution. On the contrary for Pur Pal the diffusion step is slower and the plateau is reached much later than with the other two samples. The existence of several steps in the adsorption of various pesticides on different adsorbents has been previously reported (El Bakouri et al., 2009; Hameed et al., 2009).

3.2.3. Effect of initial fenarimol concentration

Experimental fenarimol adsorption values on the three samples were fitted to various adsorption equations (Table 3).

The Langmuir equation assumes that there is no interaction between the adsorbate molecules and that the adsorption is localized in a monolayer. Therefore, once the pesticide occupies the monolayer, a saturation value is reached beyond which no further adsorption can take place. The fitting to the Langmuir equation was found to be appropriate for Pur Pal and for Sif Pal, with a plateau indicating that saturation was reached and with determination coefficients ranging from 0.887 to 0.937. The K_L values showed that adsorption of fenarimol on Pur Pal was more than

Table 4
Thermodynamic parameters for the interaction of fenarimol with raw and modified Algerian palygorskites at four temperatures.

Clays	ΔG (kJ mol^{-1})				ΔH (kJ mol^{-1})	ΔS (kJ mol^{-1} K^{-1})	R^2
	283 K	288 K	293 K	298 K			
Sif Pal	−7.48	−5.79	−4.79	−2.98	−92.79	−0.301	0.985
Pur Pal	−9.61	−8.09	−6.59	−4.84	−102.77	−0.329	0.996
Fe_2O_3 Pal	−12.05	−10.41	−7.22	−6.60	−128.41	−0.411	0.964

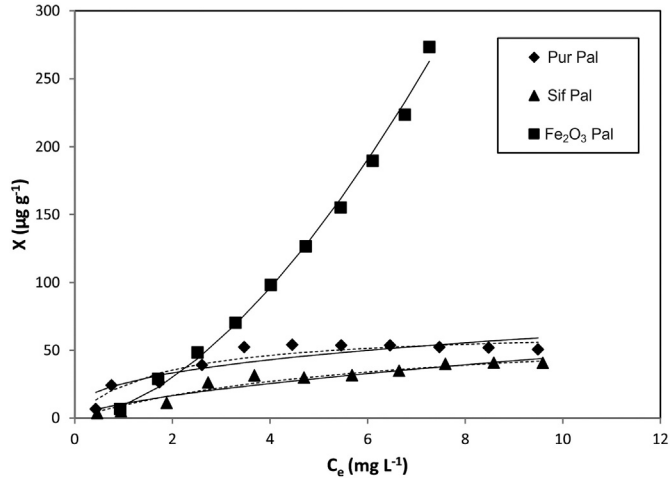

Fig. 7. Effect of initial fenarimol concentration on adsorption rates. The experimental values (symbols) are fitted to the Langmuir (dotted lines) and to the Freundlich (straight lines) equations.

3-fold higher than that of Sif Pal (Fig. 7) and the R_L values confirm that adsorption was favorable for both samples.

However the fitting to this model for the adsorption data from Fe_2O_3 Pal was not acceptable because the confidence intervals of X_{max} and K_L included negative values. Similar results have been previously reported with different pesticides on various adsorbates (De Wilde et al., 2009; Rojas et al., 2014) indicating that this model failed to describe fenarimol adsorption on this modified Pal (Table 3), either because this adsorbent exhibits a chemical heterogeneity or because monolayer adsorption was not a valid assumption for this substrate.

The Freundlich equation, which assumes a multi-layer adsorption process, fitted the experimental fenarimol adsorption data with $R^2 = 0.904$ for Sif Pal and 0.773 for Pur Pal and increased to 0.994 for Fe_2O_3 Pal.

According to this model, Pur Pal and Sif Pal would follow an L isotherm in accordance with the classification of Giles et al. (1960), with 1/n value <1, which indicates a decrease in specific adsorption sites with concentration as the adsorptive sites become occupied. For Fe_2O_3 Pal the isotherm is of an S type, with 1/n > 1, implying that adsorption increases with adsorbate concentration. This type of isotherm suggests cooperative adsorption in which weak pesticide–adsorbent interactions are presumed to occur at low aqueous concentrations, whereas at higher aqueous concentrations the adsorbed pesticide promotes further adsorption, possibly due to the creation of additional adsorptive sites through a better alignment of clay mineral platelets and/or condensation of organic compounds in clay mineral interlayer space (Li et al., 2006). However, the lower R^2 values and the higher standard errors of the estimates (not shown) for Sif and Pur Pal are an indication that for these two samples the Langmuir model better predicts the observed adsorption.

The adsorption Freundlich coefficients (K_f) suggested that the highest fenarimol adsorption corresponded to Pur Pal, but this only occurred at low pesticide concentration (Fig. 7), because of the different values of the 1/n coefficients (Table 3). Other reports have established that comparison of K_f values is not possible when the 1/n values of the isotherms differ greatly (Delgado-Moreno et al., 2010). Therefore a distribution coefficient for a $C_e = 5$ mg L^{-1} was calculated (Table 3). The values of K_d were ranged as Fe_2O_3 Pal > Pur Pal > Sif Pal, in accordance with the observed values (Fig. 7). Though fenarimol is a neutral molecule, it possesses a dipole moment (2.97 D), because it contains both negatively- and positively-charged regions (Fig. 1) (Wehtje et al., 2000). Therefore polar interactions, such as hydrogen bonding or π–π interactions, may be significant in the adsorption of fenarimol on the outer adsorbent surfaces. Additionally, due to the molecular fenarimol dimension (0.89 × 0.97 × 1.01 nm) its access to the nanotube would be restricted or even excluded, pointing to a surface phenomenon.

3.3. Thermodynamics of adsorption

The thermodynamic parameters for the adsorption of fenarimol onto the three samples of Pal were determined at various temperatures (283, 288, 293 and 298 K) (Table 4).

Negative values of ΔG at all temperatures tested suggest that fenarimol adsorption was thermodynamically favorable or a spontaneous process (Memon et al., 2008; Hameed et al., 2009). ΔG less negative values at higher temperatures imply higher driving forces of adsorption at low than at high temperature. The more negative values of ΔG for Fe_2O_3 Pal are an indication that fenarimol adsorption is more favorable in this sample (Cestari et al., 2007). It may be deduced from the negative values of the enthalpy (ΔH) for the three materials that the adsorption process is exothermic in nature (Memon et al., 2008) supported by the fact that fenarimol adsorption decreased with increasing temperature. Typically ΔH for chemical adsorption ranges between −40 and −400 kJ mol^{-1}. Consequently, fenarimol adsorption on the three adsorbents can be considered as chemical in nature. The values of the entropy (ΔS) are all negative for the interaction of fenarimol, which confirms that randomness decreased at the solid–solution interface during pesticide fixation on the adsorbent surfaces.

3.4. Desorption stability

As it may be deduced from the desorption behavior (Fig. 8), the initial relative amount of desorbed fenarimol was inversely related with its adsorption on each sample, higher for Sif Pal, followed by Pur Pal and finally by Fe_2O_3 Pal. Desorbed fenarimol from Sif Pal and from Fe_2O_3 Pal remained fairly constant during the studied period, reflecting the stability of both adsorbents for retaining the pesticide. However, for Pur Pal the amount of desorbed fenarimol increased with time, an indication that the pesticide became more available with time. Therefore, though the Pur Pal was able to retain the pesticide to a remarkable extent (Fig. 8) the high retention was only shown to be stable for Fe_2O_3 Pal during the studied period.

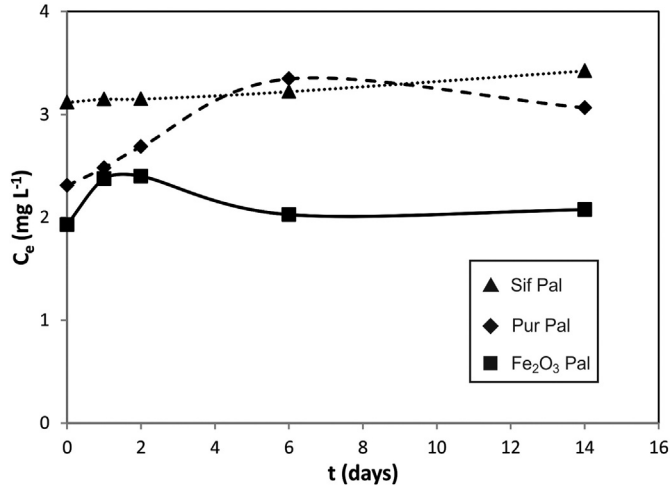

Fig. 8. Evolution with time of fenarimol desorption from the three adsorbents.

4. Conclusions

The present study shows that the fungicide fenarimol can be selectively adsorbed by Fe_2O_3 Pal that greatly increased the fenarimol retention capacity (70%) when compared to Sif Pal (11%) and Pur Pal (50%). The adsorption equilibrium data were analyzed using two adsorption models, and the results show that the adsorption behavior

of fenarimol by Sif Pal and Pur Pal could be described by both Langmuir and Freundlich models, providing high R^2 values while adsorption on Fe_2O_3 Pal could be only explained by the Freundlich approach. The adsorption kinetics was rapid, being the equilibrium reached in all cases in several hours. Faster diffusion of the pesticide into Fe_2O_3 Pal was found, being the adsorption rates limited in all cases by diffusion into micropores. In addition the adsorption capacity of fenarimol remained stable for at least two weeks, showing that this material could be used to provide a safe and sustained fenarimol removal. Once the pesticide is adsorbed on Fe_2O_3 Pal, the polluted material could be selectively removed by using a magnet.

Symbol abbreviations

1/n	Freundlich constant
C	constant of intraparticle diffusion ($\mu g\ g^{-1}$)
C_e	equilibrium concentration ($mg\ L^{-1}$)
CEC	cation exchange capacity $meq_+/100\ g$
Fe_2O_3 Pal	Algerian palygorskite coated with magnetic iron oxide
k_1	rate constant for the first-order kinetics (min^{-1})
k_2	rate constant for the pseudo second-order kinetics ($g\ \mu g^{-1}\ min^{-1}$)
K_f	Freundlich constant ($mg^{1-1/n}\ mL^{1/n}\ kg^{-1}$)
K_L	Langmuir constant ($L\ mg^{-1}$)
k_p	intraparticle diffusion rate constant ($\mu g\ g^{-1}\ min^{-1/2}$)
Pur Pal	purified Algerian palygorskite
R_L	dimensionless separation factor
Sif Pal	raw Algerian palygorskite rich in dolomite
X_e	amount adsorbed at equilibrium ($\mu g\ g^{-1}$)
X_{max}	maximum adsorbed amount ($\mu g\ g^{-1}$)
X_t	adsorbed amount at time t ($\mu g\ g^{-1}$)
ΔG	Gibbs free energy ($kJ\ mol^{-1}$)
ΔH	enthalpy ($kJ\ mol^{-1}$)
ΔS	entropy ($kJ\ mol^{-1}\ K^{-1}$)

Acknowledgments

The authors acknowledge funding from the FP7 Marie-Curie Action IRSES-MEDYNA action under GA PIRSES-GA-2013-6125, and the suggestions made by Faiza Bergaya and Massimo Setti.

References

Azejjel, H., del Hoyo, C., Draoui, K., Rodríguez-Cruz, M.S., Sánchez-Martín, M.J., 2009. Natural and modified clays from Morocco as sorbent of ionizable herbicides in aqueous medium. Desalination 3, 1151–1158.
Belaroui, L.S., Dali Youcef, L., Ouali, A., Bengueddach, A., Lopez Galindo, A., 2014. Mineralogical and chemical characterization of palygorskite from East-Algeria. Rev. Soc. Esp. Miner., Macla n° 19.
Bradley, W.F., 1940. The structure scheme of attapulgite. Am. Miner. 25, 405–410.
Cabizza, M., Dedola, F., Satta, M., 2012. Residues behavior of some fungicides applied on two greenhouse tomato varieties different in shape and weight. J. Environ. Sci. Health B 47, 379–384.
Casal, B., Merino, J., Serratosa, J.M., Ruiz-Hitzky, E., 2001. Sepiolite and palygorskite based materials for the photo- and thermal-stabilization of pesticides. Appl. Clay Sci. 18, 245–254.
Cestari, A.R., Vieira, E.F.S., Vieira, G.S., Almeida, L.E., 2007. Aggregation and adsorption of reactive dyes in the presence of an anionic surfactant on mesoporous aminopropyl silica. J. Colloid Interface Sci. 309, 402–411.
Chen, H., Zhao, J., 2009. Adsorption study for removal of Congo red anionic dye using organo-attapulgite. Adsorption 15, 381–389.
Dali Youcef, L., 2012. Purification et caractérisation de l'attapulgite Algérienne. Application à l'adsorption du bleu de methylene, Memoire of Magister. University from Oran (106 pp.).
Daou, T.J., Pourroy, G., Begin-Colin, S., Greneche, J.M., Ulhaq-Bouillet, C., 2006. Hydrothermal synthesis of monodisperse magnetite nanoparticles. Chem. Mater. 18, 4399–4404.
De Wilde, T., Spanoghe, P., Ryckeboer, J., Jaeken, P., Springael, D., 2009. Sorption characteristics of pesticides on matrix substrates used in biopurification systems. Chemosphere 75, 100–108.
Delgado-Moreno, L., Peña, A., Almendros, G., 2010. Contribution by the different soil organic fractions to triazines sorption in Calcaric Regosol amended with raw and biotransformed olive cake. J. Hazard. Mater. 174, 93–99.
El Bakouri, H., Usero, J., Morillo, J., Rojas, R., Ouassini, A., 2009. Drin pesticides removal from aqueous solutions using acid-treated date stones. Bioresour. Technol. 100, 2676–2684.
Fauconnier, N., 1996. Adsorption de ligands organiques sur des particules de maghemite en vue d'applications biomédicales. PhD of University from Paris 6.
Fernandes de Oliveira, M., Johnston, C.T., Premachandra, G.S., Teppen, B.J., Li, H., Laird, D.A., Zhu, D., Boyd, S.A., 2005. Spectroscopic study of carbaryl sorption on smectite from aqueous suspension. Environ. Sci. Technol. 39, 9123–9129.
Fernández-Bayo, J.D., Nogales, R., Romero, E., 2008. Evaluation of the sorption process for imidacloprid and diuron in eight agricultural soils from Southern Europe using various kinetic models. J. Agric. Food Chem. 56, 5266–5272.
Fernández-Saavedra, R., Aranda, P., Ruiz-Hitzky, E., 2004. Template synthesis of carbon nanofibers from polyacrylonitrile using sepiolite. Adv. Funct. Mater. 14, 77–82.
Freundlich, H.M.F., 1906. Over the adsorption in solution. J. Phys. Chem. 57, 385–470.
Fu, R., Jin, X., Liang, J., Zheng, W., Zhuang, J., Yang, W., 2011. Preparation of nearly monodispersed Fe_3O_4/SiO_2 composite particles from aggregates of Fe_3O_4 nanoparticles. J. Mater. Chem. 21, 15352–15356.
Giles, C.H., McEwan, T.H., Nakhwa, S.N., Smith, D., 1960. Studies in adsorption. Part XI. A system of classification of solution adsorption isotherms, and its use in diagnosis of adsorption mechanisms and in measurement of specific surface areas of solids. J. Chem. Soc. 3, 3973–3993.
Grasset, F., Mornet, S., Demourgues, A., Portier, J., Bonnet, J., Vekris, A., Duguet, E., 2001. Synthesis, magnetic properties, surface modification and cytotoxicity evaluation of $Y_3Fe_{5-x}Al_xO_{12}$ ($0 \le x \le 2$) garnet submicron particles for biomedical applications. J. Magn. Magn. Mater. 234, 409–418.
Grasset, F., Labhsetwar, N., Li, D., Park, D.C., Saito, N., Haneda, H., Cador, O., Roisnel, T., Mornet, S., Duguet, E., Portier, J., Etourneau, J., 2002. Synthesis and magnetic characterization of zinc ferrite nanoparticles with different environments: powder, colloidal solution and zinc ferrite-silica core–shell nanoparticles. Langmuir 18, 8209–8216.
Hameed, B.H., Salman, J.M., Ahmad, A.L., 2009. Adsorption isotherm and kinetic modelling of 2,4-D pesticide on activated carbon derived from date stones. J. Hazard. Mater. 163, 121–126.
Hernández-Soriano, M.C., Mingorance, M.D., Peña, A., 2012. Desorption of two organophosphorous pesticides from soil with wastewater and surfactant solutions. J. Environ. Manag. 95, S223–S227.
Ho, Y.S., McKay, G., 2000. The kinetics of sorption of divalent metal ions onto sphagnum moss peat. Water Res. 34, 735–742.
Ho, Y.S., Wasse, D.A.J., Forster, C.F., 1996. Kinetic studies of competitive heavy metal adsorption by sphagnum moss peat. Environ. Technol. 17, 71–77.
Kibbey, T.C.G., Hayes, K.F., 1993. Partitioning and UV absorption studies of phenanthrene on cationic surfactant-coated silica. Environ. Sci. Technol. 27, 2168–2173.
Lagergren, S., 1898. Zur Theorie der sogennanten Adsorption gelöster Stoffe. Kungliga Svenska Vetenskapsakademiens. Handlingar 24, 1–39.
Langmuir, I., 1918. The adsorption of gases on plane surface of glass, mica and platinum. J. Am. Chem. Soc. 40, 1361–1403.
Lefebvre, S., 1996. Particules magnétiques de granulométrie controlée enrobée de tensioactifs et de polymères: ferrofluide et couches magnétiques. PhD University Paris 6.
Li, H., Teppen, B.J., Laird, D.A., Johnston, C.T., Boyd, S.A., 2006. Effects of increasing potassium chloride and calcium chloride ionic strength on pesticide sorption by potassium- and calcium-smectite. Soil Sci. Soc. Am. J. 70, 1889–1895.
Massart, R., 1982. Preparation of aqueous magnetic liquids in alkaline and acidic media. IEEE Trans. Magn. 17, 1247–1248.
Memon, G.Z., Bhanger, M.I., Qkhtar, M., Talpur, F.N., Memon, J.R., 2008. Adsorption of methyl parathion pesticide from water using watermelon peels as a low cost adsorbent. Chem. Eng. J. 138, 616–621.
Mingorance, M.D., Barahona, E., Fernández-Gálvez, J., 2007. Guidelines for improving organic carbon recovery by the wet oxidation method. Chemosphere 68, 409–413.
Mornet, S., Vekris, A., Bonnet, J., Duguet, E., Grasset, F., Choy, J.-H., Portier, J., 2000. DNA-magnetite nanocomposite materials. Mater. Lett. 42, 183–188.
Park, M., Han, J., Ko, J.-J., Lee, W.-S., Yoon, T.K., Lee, K., Bae, J., 2011. Maternal exposure to fenarimol promotes reproductive performance in mouse offspring. Toxicol. Lett. 205, 241–249.
Peña, A., Mingorance, M.D., Guzmán, I., Sánchez, L., Fernández-Espinosa, A.J., Valdés, B., Rossini-Oliva, S., 2014. Protecting effect of recycled urban wastes (sewage sludge and wastewater) on ryegrass against the toxicity of pesticides at high concentrations. J. Environ. Manag. 142, 23–29.
Peng, X., Wang, J., Fan, B., Luan, Z., 2009. Sorption of endrin to montmorillonite and kaolinite clays. J. Hazard. Mater. 168, 210–214.
Rivagli, E., Pastorello, A., Sturini, M., Maraschi, F., Speltini, A., Zampori, L., Setti, M., Malavasi, L., Profumo, A., 2014. Clay minerals for adsorption of veterinary FQs: behavior and modelling. J. Environ. Chem. Eng. 2, 738–744.
Rodríguez-Liébana, J.A., Mingorance, M.D., Peña, A., 2014a. Pesticide mobility and leachate toxicity in two abandoned mine soils. Effect of organic amendments. Sci. Total Environ. 497–498, 561–569.
Rodríguez-Liébana, J.A., Mingorance, M.D., Peña, A., 2014b. Role of irrigation with raw and artificial wastewaters on pesticide desorption from two Mediterranean calcareous soils. Water Air Soil Pollut. 225, 2049.
Rojas, R., Vanderlinden, E., Morillo, J., Usero, J., El Bakouri, H., 2014. Characterization of sorption processes for the development of low-cost pesticide decontamination techniques. Sci. Total Environ. 488–489, 124–135.
Saha, A., Shabeer, A.T.P., Gajbhiye, V.T., Gupta, S., Kumar, R., 2013. Removal of mixed pesticides from aqueous solutions using organoclays: evaluation of equilibrium and kinetic model. Bull. Environ. Contam. Toxicol. 91, 111–116.
Serratosa, J.M., 1978. Surface properties of fibrous clay minerals (palygorskite and sepiolite). In: Mortland, M.M., Farmer, V.C. (Eds.), Developments in SedimentologyInternational Clay Conference 27. Elsevier, Amsterdam, pp. 99–109.

Shaarani, F.W., Hameed, B.H., 2010. Batch adsorption of 2,4-dichlorophenol onto activated carbon derived from agricultural waste. Desalination 255, 159–164.
Suarez Barrios, M., Flores González, L.V., Vicente Rodríguez, M.A., Martin Pozas, J.M., 1995. Acid activation of a palygorskite with HCl: development of physico-chemical textural and surface properties. Appl. Clay Sci. 10, 247–258.
Tomlin, C.D.S., 2003. The Pesticide Manual. 13th edition. British Crop Protection Council, UK (1344 pp.).
Travis, C.C., Entier, E.L., 1981. A survey of sorption relationships for reactive solutes in soil. J. Environ. Qual. 10, 8–17.
Villaverde, J., van Beinum, W., Beulke, S., Brown, C.D., 2009. The kinetics of sorption by retarded diffusion into soil aggregate pores. Environ. Sci. Technol. 43, 8227–8232.
Watermann, B.T., Albanis, T.A., Dagnac, T., Gnass, K., Kusk, K.O., Sakkas, V.A., Wollenberger, L., 2013. Effects of methyltestosterone, letrozole, triphenyltin and fenarimol on histology of reproductive organs of the copecod *Acartia tonsa*. Chemosphere 92, 544–554.
Weber, W.J., Morris, J.C., 1963. Kinetics of adsorption on carbon from solution. J. Sanit. Eng. Div. 89, 31–60.
Wehtje, G., Walker, R.H., Shaw, J.N., 2000. Pesticide retention by inorganic soil amendments. Weed Sci. 48, 248–254.
Wightwick, A.M., Bui, A.D., Zhang, P., Rose, G., Allinson, M., Myers, J.H., Reichman, S.M., Menzies, N.W., Pettigrove, V., Allinson, G., 2012. Environmental fate of fungicides in surface waters of a horticultural-production catchment in Southeastern Australia. Arch. Environ. Contam. Toxicol. 62, 380–390.
World Health Organization, 2009. The WHO recommended classification of pesticides by hazard Data available online at, http://www.who.int/ipcs/publications/pesticides_hazard_2009.pdf (accessed April 2015).